

Chloride-mediated selective electrosynthesis of ethylene and propylene oxides at high current density

Wan Ru Leow^{1*}, Yanwei Lum^{1,2*}, Adnan Ozden³, Yuhang Wang¹, Dae-Hyun Nam¹, Bin Chen¹, Joshua Wicks¹, Tao-Tao Zhuang¹, Fengwang Li¹, David Sinton³, Edward H. Sargent^{1†}

¹Department of Electrical and Computer Engineering, University of Toronto, 35 St George Street, Toronto, ON M5S 1A4, Canada. ²Institute of Materials Research and Engineering, Agency for Science, Technology and Research (A*STAR), 2 Fusionopolis way, Innovis, Singapore 138634, Singapore. ³Department of Mechanical and Industrial Engineering, University of Toronto, 5 King's College Road, Toronto, ON M5S 3G8, Canada.

*These authors contributed equally to this work.

†Corresponding author. Email: ted.sargent@utoronto.ca

Commented [CF1]: Note, title was updated at editor's suggestion

Author: Please check all editing changes carefully and respond on the galley to the queries to you that are shown in balloons in the right margins. Inserted text is blue; deleted text is red with strike-through marks. Please check all equations in the galleys to be sure that they are set correctly, mark all changes directly on the downloaded galley—not this document—and return the galleys to me. Thank you.

Chris Filiatreau
Content Production Editor
Science
1200 New York Ave., NW
11th Floor
Washington, DC 20005
Tel: 202-326-6742
E-mail: cfiliatr@aaas.org

Chemicals manufacturing consumes large amounts of energy and is responsible for a **significant** **substantial** portion of global carbon emissions. Electrochemical systems that produce the desired compounds **by** using renewable electricity offer a route to lower carbon emissions in the chemicals sector. Ethylene oxide is among the world's most abundantly produced commodity chemicals ~~due to~~ **because of** its importance in the plastics industry, notably for manufacturing polyesters and polyethylene terephthalates (**PET**). ~~Here w~~ **We apply-applied** an extended heterogeneous:homogeneous interface, using chloride as a redox mediator at the anode, to facilitate the selective partial oxidation of ethylene to ethylene oxide. ~~w~~ **We achieved** current densities of 1 **ampere per square centimeter** A/cm^2 , Faradaic efficiencies of ~70%, and product specificities of ~97%. When run at 300 **milliamperes per square centimeter** mA/cm^2 for 100 hours, the system maintained a 71(\pm 1)% Faradaic efficiency throughout.

Commented [CF2]: Science reserves "significant" to denote statistical significance.

In the United States, chemical manufacture accounts for 28% of total industrial energy demand (1). At present, this demand is largely met by the consumption of fossil fuels, resulting in ~~significant~~ **substantial carbon dioxide** (CO₂) emissions (2, 3); a recent report showed that the plastics industry alone releases 1.8 billion metric tons of CO₂ per year; and that replacing fossil fuels–based production methods with ones powered ~~with~~ **using** renewable energy offers a route to reduce net greenhouse gas emissions associated with plastics manufacture (4).

One attractive strategy involves ~~the developing~~ **development of** electrochemical systems that produce the necessary raw materials **by** using renewable electricity (5–8). Ethylene oxide is used in the manufacture of plastics, detergents, thickeners, and solvents (9) and is among the world’s top 15 most abundantly produced chemicals at ~20 million metric tons per ~~annum~~ **year** (10, 11). At present, it is manufactured through the ~~silver~~ (Ag)–catalyzed direct oxidation of ethylene at high temperature and pressure (200° ~~to~~ 300°C and 1- ~~to~~ 3 MPa). This process generates 0.9 ~~tons~~ of CO₂ per ton **of** ethylene oxide produced, with ~~over~~ **more than** half attributed to the complete combustion of ethylene; and the balance arising from temperature-control units (Fig. 1A), which today are fossil- fuel–powered (12).

The contribution from the complete oxidation of ethylene all the way to CO₂ is a result of the mechanism relied ~~upon~~ in direct ethylene oxidation: ~~e~~ **One** ethylene reacts with one oxygen (**O**) atom from Ag-adsorbed dioxygen to form ethylene oxide, leaving behind the remaining Ag-adsorbed ~~oxygen~~ **O** atom, and this oxidizes ethylene all the way to CO₂. ~~Since~~ **It takes 6-six** ~~oxygen~~ **O** atoms for the complete combustion of ~~1-one~~ ethylene molecule; this means that, in the best case, for every ~~6-six~~ molecules of ethylene converted to ethylene oxide, ~~1-one~~ molecule of ethylene will be completely combusted to CO₂, thus limiting the product specificity to a theoretical upper limit of 85.7% (9). Here, specificity refers to the percentage of reacted substrate (ethylene) that goes toward the desired product (ethylene oxide).

Additionally, fossil-powered systems are typically used to maintain a stable temperature profile in order to suppress thermal runaway in this highly exothermic reaction.

~~Here~~ **w** **We** pursued an electrochemical approach to the production of ethylene oxide; to address both the first problem (limited product specificity) and the second (the need to reduce the use of fossil energy sources in powering systems). We sought a highly selective electrochemical route, pursuing the electrooxidation of ethylene to ethylene oxide with high product specificity and Faradaic efficiency under ambient conditions as a means to contribute to lowering CO₂ emissions in the production of this chemical (Fig. 1B) (13, 14).

The electrosynthesis of ethylene oxide involves the partial oxidation of ethylene, an anodic reaction. Reactions of this nature at high current density and Faradaic efficiency are hampered by two challenges. First, the large positive potentials necessary can lead to uncontrolled over-oxidation, generating undesired by-products such as CO₂. Currently, reported anodic upgrading reactions such as the oxidation of 5-hydroxymethylfurfural (15–17), alcohol (18–20), and glycerol (21–23) are conducted at low current densities (<100 mA/cm²) to maximize Faradaic efficiencies toward the target product (Fig. 1C). However, the production of industrially- relevant quantities of the product at such low current densities would require unreasonably high electrolyzer surface areas, leading to high capital costs per unit of productivity (Fig. 1D). Second, if the reactant (ethylene) has limited solubility in the aqueous electrolyte, the system quickly becomes mass- transport–limited, resulting in poor Faradaic efficiency at high current densities.

Commented [CF3]: Correct that “metric ton” is meant here and throughout (in which case, the shortened “ton” is fine, after previous initial use of “metric ton”)? If not, please convert relevant values to the metric ton.

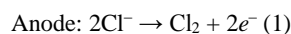
We took the view that a selective production strategy could avoid directly oxidizing the organic reactant molecules on the electrode surface so as to prevent over-oxidation at high current densities. We reasoned that a redox mediator that facilitates the indirect exchange of electrons between the electrode and the substrate molecules would allow this. Furthermore, in such a scheme, the space in which the reaction takes place is not limited to the planar electrode:electrolyte interface; but ~~in fact~~ extends into the bulk electrolyte, constituting an extended heterogeneous:homogeneous interface (Fig. 2A) that overcomes mass transport limitations. Using this strategy, we demonstrated ethylene oxide production at high current density (up to 1 A/cm²), Faradaic efficiency (~70%), and product specificity (~97%).

Initially, we attempted to oxidize ethylene directly to ethylene oxide using a nanostructured palladium (Pd) anode (Fig. S2A). This approach was based on a recent study in which olefins such as propylene were oxidized at low current densities (24); but did not translate to the high current densities; at 300 mA/cm², a negligible Faradaic efficiency was obtained toward ethylene oxide (Fig. S2B). Operating at this high current density resulted in dissolution of the Pd anode, as can be observed from the rapidly increasing potential with time (Fig. S2C). Additionally, the use of organic mediators such as TEMPO [(2,2,6,6-tetramethylpiperidin-1-yl)oxyl] (15, 2825) and NHPI (N-hydroxyphthalimide) (2926, 3027) — a method to obtain high selectivities for partial oxidation products at the anode — failed in the generation of ethylene oxide and yielded instead only small amounts of acetate (Fig. 2B).

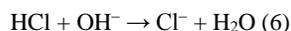
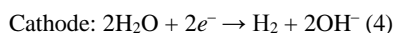
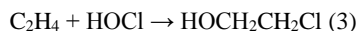
Historically, ethylene oxide was produced from ethylene through the addition of aqueous chlorine to form ethylene chlorohydrin, followed by dehydrochlorination with calcium hydroxide to generate ethylene oxide (9). However, the high cost associated with consuming stoichiometric amounts of chlorine and hydroxide, as well as disposal of the water medium, has lowered interest in this process. We postulated that chloride (Cl⁻) could be a redox mediator at the anode with extended heterogeneous:homogeneous interfaces. The Cl⁻ could thereby buffer ethylene from uncontrolled oxidation and facilitate ethylene oxide production.

This idea was tested in a flow-cell setup with 1.0 M potassium chloride (KCl) electrolyte, in which ethylene was continuously sparged into the anolyte, with platinum (Pt) foil as the working electrode (anode), nickel (Ni) foam as the counter electrode (cathode), and Ag/AgCl (3.0 M KCl) as the reference electrode (Fig. S3). The geometric surface area of the anode used was 1 cm², and the catholyte and anolyte volumes were both 25 ml. An anion exchange membrane (AEM) separated the anolyte and catholyte chambers. To determine the Faradaic efficiency, product quantification was carried out by means of high-performance liquid chromatography (HPLC); see (supplementary materials, Materials and Methods for more details). Unless otherwise stated, all electrolysis experiments were run for a duration of 1 hour.

Experiments were first carried out at 300 mA/cm². ~~Based on~~ On the basis of prior studies (328), in this process, Cl⁻ is oxidized to Cl₂ at the Pt anode (Eq. 1); *e* is the charge on the electron, which disproportionates in the aqueous environment to form hypochlorous and hydrochloric acid (HOCl and HCl, respectively) (Eq. 2) (329, 330); HOCl then reacts with ethylene dissolved in the electrolyte to form ethylene chlorohydrin (HOCH₂CH₂Cl) (Eq. 3). Because HCl is not consumed, the pH of the anolyte becomes acidic over the course of the electrolysis (pH 1.1):



Commented [CF4]: Several references were cited out of numerical order, requiring renumbering; please check all references and in-text callouts carefully.



The final step involves addition of hydroxide (OH^-), which then reacts with ethylene chlorohydrin to yield the desired ethylene oxide and regenerate Cl^- (3428). The hydrogen evolution reaction (Fig. S4) at the cathode during electrolysis generates the necessary OH^- (Eq. 4), while-whereas the AEM prevents complete mixing of the catholyte and the anolyte. Consequently, at the end of electrolysis, the pH of the catholyte becomes alkaline, with a pH value of 13.8. This means that by mixing the catholyte and anolyte output streams (performed post-after electrolysis), ethylene oxide can be generated from the reaction between ethylene chlorohydrin and OH^- (Eq. 5 and Fig. 2B). At the same time, the HCl generated (Eq. 2) is also neutralized by OH^- (Eq. 6).

The formation of ethylene chlorohydrin in the anolyte and subsequent generation of ethylene oxide in the mixing step were confirmed through ^1H nuclear magnetic resonance (NMR) (Fig. S5). We performed the same experiments but using carbon-13-labeled ethylene ($^{13}\text{C}_2\text{H}_4$): ^{13}C NMR and ^1H NMR results confirm that the products we observed are-were indeed due to the partial oxidation of ethylene (Fig. 2C and Fig. S5). We note that in principle, a cation exchange membrane would be better in preventing crossover of OH^- (Fig. S6A). However, this would lead to a continuous decrease in electrolyte (anolyte) conductivity during operation, resulting in lowered performance (see Fig. S6B). In sum, this system enables the generation of ethylene oxide in a single electrolyzer under ambient temperatures and pressures: ethylene, water, and electricity are the consumables (Eq. 7).

Using this method, we achieved a Faradaic efficiency of 70-(±1)-% toward ethylene oxide (Fig. 2D) with 1.0 M KCl at 300 mA/cm². This corresponds to 3.9 mmol of ethylene oxide produced after 1 hour of electrolysis. Similar Faradaic efficiencies of 71-(±1)-% and 70-(±1)-% are maintained even at current densities of 500 and 800 mA/cm², respectively (Fig. 2D). A possible explanation for the missing charge could be O_2 evolution or complete oxidation of ethylene to form CO_2 ; however, when we performed gas chromatography on the output gas stream, we did not detect O_2 nor CO_2 . We note that the product specificity has a value of 97%; ethylene conversion to other products (e.g., such as CO_2) was not observed, and the remaining specificity was due to incomplete conversion of ethylene chlorohydrin to ethylene oxide (Eq. 5).

We instead hypothesized that the missing charge could be due to unreacted chlorine or hypochlorite species in the electrolyte; this was confirmed by using iodometric titration (see Fig. S7 and Table S1). We note that Pt and iridium oxide/titanium (IrO_2/Ti) anodes resist corrosion even at high chlorine concentrations during the chlor-alkali process (3431). A continuous flow reactor process could be adopted (as opposed to the current batch reactor mode), whereby in which portions of the electrolyte are periodically siphoned off for ethylene oxide extraction. In this case, the electrolyte would be continuously replenished by fresh or regenerated solution, thereby preventing excessive buildup of these corrosive species.

The method could also be used for the epoxidations of other olefins; for instance example, when we replaced ethylene with propylene, Faradaic efficiencies were 69 to

Commented [CF5]: We reserve using the solidus to denote a ratio; "or" correct as meant here?

71% toward propylene oxide—a commodity chemical with a market of 10 million tons per annum-year market in the plastics industry (3532)—at current densities of 300 to 800 mA/cm² (Fig. 2E).

We performed a techno-economic analysis (TEA) to identify conditions that could enable the profitable synthesis of a renewable-energy-powered anodic partial oxidation of ethylene to ethylene oxide (fig. S1) (full details of the TEA are available in the see-Ssupplementary Mmaterials-for full details of TEA, Fig. S1). For the TEA, we set a base electricity cost of 10 ¢/kWh, which is at least twice the average present-day industrial electricity cost (fig. S8) (6) (Fig. S8). Sensitivity analysis reveals that the greatest dependency of the plant-gate leveled cost is on electrochemical parameters such as current density and Faradaic efficiency (Fig. S8; see the range of values considered for each parameter is provided in Table S2-for range of values considered for each parameter). Based on the basis of the current market price per ton of ethylene oxide and the corresponding quantity of hydrogen produced at the cathode, we determined that for a current density of 300 mA/cm², the minimum energy efficiency required for the renewable energy-powered process to be profitable is ~30%. We also calculated the minimum energy efficiencies required to be profitable for different electricity costs up to 20 ¢/kWh, showing profitable regions as a function of energy efficiency and electricity cost (Fig. 3A). Similarly, this was also calculated for the electrosynthesis of propylene oxide from propylene (Fig. S9).

The sensitivity analysis of in Fig. S8 revealed that the plant-gate leveled cost is sensitive to electrochemical parameters such as Faradaic efficiency and cell potential. To reduce energy cost, we sought to increase the energy efficiency of the reaction by varying the electrolyte concentration while operating at 300 mA/cm². We began at a lower Cl⁻ concentration (0.5 M); however, oxygen evolution from water then dominates the anodic reaction, resulting in a low Faradaic efficiency of 30(±1)% and energy efficiency of 11(±1)% (Fig. 3B). As the Cl⁻ concentration increases (1.0 M and 2.0 M), the overpotential decreases [(5.8(±0.2) V and 4.0(±0.1) V)] due to because of improved Cl⁻ oxidation kinetics and increased electrolyte conductivity, leading to increased Faradaic efficiencies [70(±1)% and 67(±1)%] and half-cell energy efficiencies [18(±1)% and 27(±1)%]. At 3.5 M, however, the energy efficiency was unimproved at 26(±1.9)% as because the reduced potential [(3.6(±0.2) V)] was negated by a slight decrease in Faradaic efficiency to 55(±1)%, likely because the increased Cl⁻ concentration is unfavorable for the disproportionation of Cl₂ into HOCl and HCl (Eq. 2). Thus, based on the basis of the corresponding plant-gate leveled costs, we determined the optimal Cl⁻ concentration to be 2.0 M. In this work, all potentials are reported vs. versus Ag/AgCl and are not infrared (IR)-corrected.

Even at the optimal Cl⁻ concentration, the renewable electricity-based plant-gate leveled cost remains higher than the current market price per ton of ethylene oxide and the corresponding quantity of hydrogen (Fig. 3B). We turned to the working electrode (catalyst) as another degree of freedom to decrease the overpotential. We prepared IrO₂ deposited on Ti mesh (Fig. 3C and Fig. S10) using a dip coating and thermal decomposition procedure (3633). X-ray photoelectron spectroscopy (XPS) results confirmed the presence of Ir in a +4 oxidation state (Fig. S10, A- to C). Scanning electron microscopy (SEM) images show the microscale mesh structure of the IrO₂-coated Ti mesh (Fig. S10D). Energy-dispersive X-ray spectroscopy (EDX) confirmed the presence of Ir and O on the Ti mesh, indicating the loading of IrO₂ on Ti (Fig. 3C). X-ray diffraction (XRD) was also performed on the IrO₂ coating as well as the bare Ti

mesh (Fig. S10E). Additionally, **transmission electron microscopy (TEM)** images of the IrO₂ were acquired (Fig. S10, F- and G). Using this catalyst, we lowered the required applied potential from 3.4(±0.1) V to 3.0(±0.1) V, thus further raising the half-cell energy efficiency to 30(±1)-% at 300 mA/cm².

Having optimized the electrochemical system, we measured the energy efficiencies and plant-gate levelized costs under different current densities to determine the most economical conditions for industrial manufacturing (Fig. 3D). Faradaic efficiencies were maintained even at a current density of 1 A/cm² [(60(±4)-%)]. However, a much higher potential of 6.5(±0.5) V was required to drive the larger current, leading to a low half-cell energy efficiency [(12(±1)-%)]. On the other hand, the half-cell energy efficiency is high at 38.3(±0.1)-% under 50 mA/cm²; thus, the electricity cost per ton of ethylene oxide is at the lowest. However, the high capital cost associated with electrolyzer surface area resulted in an uneconomical plant-gate levelized cost. The plant-gate levelized cost is the lowest at 300 mA/cm², with good energy efficiency of 30 (±1)-% and acceptably low capital costs.

~~Based on~~ **On the basis of** this analysis, we investigated the stability of the catalyst system at the most profitable current density of 300 mA/cm², during which portions of the electrolyte were periodically removed for analysis and replaced with fresh electrolyte. The system maintained a stable applied potential of 2.86(±0.02) V and Faradaic efficiency averaging 71(±0.6)-% for 100 hours continuously (Fig. 4A). Post-reaction analysis of the anode through SEM and EDX revealed no obvious structural changes of the Ti mesh surface nor loss of IrO₂ (Fig. S11). The method **significantly** outperforms other reported anodic upgrading reactions in current density, product generation rate, and reported operation time, while maintaining high Faradaic efficiency and ethylene oxide specificity (Fig. 4B). The specificity in this case is 95%; we did not observe the conversion of ethylene to other products (e.g., such as CO₂). This high specificity is important in an industrial process, ~~since~~ **because** the ethylene will likely be continuously recirculated to maximize usage.

~~Finally~~ **Last**, we sought to develop an integrated system to perform the electrosynthesis of ethylene oxide from CO₂ (rather than ethylene) as the starting feedstock. This provides a route to directly use renewable electricity for recycling CO₂ into a valuable commodity chemical. In this integrated system, CO₂ reduction to ethylene is first performed **by** using a membrane electrode assembly (MEA) in a gas diffusion configuration, with O₂ evolution from water as the corresponding anodic reaction (Fig. 4C). The MEA comprises a copper nanoparticle/copper/polytetrafluoroethylene (Cu NPs/Cu/PTFE) cathode and an IrO₂/Ti mesh anode separated by an AEM, through which 0.1 M **potassium bicarbonate (KHCO₃)** anolyte was continuously circulated. The operating current density was kept at 240 mA/cm², and the ethylene Faradaic efficiency was generally maintained at 43 to 52% (Fig. 4D). **We measured** ~~the~~ **the** flow rate of the output gas ~~was measured~~ using a flow meter at the cathode gas outlet, and **the output gas was** directly sparged into the anolyte of the ethylene-to-ethylene oxide flow cell (operated at 300 mA/cm²) without further purification.

~~Through~~ **With** this method, we achieved a Faradaic efficiency of 45% toward ethylene oxide under a gas flow rate of 6 **standard cubic centimeters per minute (sccm)** (Fig. 4D), despite the presence of other easily oxidizable gases such as H₂ and CO relative to ethylene (23% H₂, 12% CO, and 12% ethylene); ~~see~~ (Fig. S12; and Tables S3- and S4). Oxidation of these gases requires direct contact with the anode, whereas ethylene oxidation is mediated by the extended heterogeneous:homogeneous interface and thus occurs in the bulk electrolyte at a much

Commented [CF6]: Is statistical significance meant here?

higher rate. The Faradaic efficiency toward ethylene oxide was reduced at a higher gas flow rate ~~due~~ owing to lowered ethylene concentration in the MEA output stream (see Fig. S12; and Tables S3- and S4). However, decreasing the flow rate even further (3 sccm) resulted in a lowered Faradaic efficiency toward ethylene in the MEA. This reduces the ethylene supply available for conversion in the flow cell, resulting in a drop in the Faradaic efficiency toward ethylene oxide. Thus, both concentration and molar quantity of ethylene in the MEA output stream are important determinants for the Faradaic efficiency toward ethylene oxide in the flow cell.

This demonstration shows the viability of an integrated system for complete CO₂-to-ethylene oxide conversion. Further improvements are expected by optimizing the ethylene Faradaic efficiency and single-pass conversion in the MEA.

References and Notes

1. U.S. Energy Information Administration (EIA), "Energy use in industry," in *Use of Energy Explained* (EIA, 2019).
2. S. Chu, Y. Cui, N. Liu, The path towards sustainable energy. *Nat. Mater.* **16**, 16–22 (2016).
3. Z. W. Seh, J. Kibsgaard, C. F. Dickens, I. Chorkendorff, J. K. Nørskov, T. F. Jaramillo, Combining theory and experiment in electrocatalysis: Insights into materials design. *Science* **355**, eaad4998 (2017).
4. J. Zheng, S. Suh, Strategies to reduce the global carbon footprint of plastics. *Nat. Clim. Chang.* **9**, 374–378 (2019).
5. P. De Luna, C. Hahn, D. Higgins, S. A. Jaffer, T. F. Jaramillo, E. H. Sargent, What would it take for renewably powered electrosynthesis to displace petrochemical processes? *Science* **364**, eaav3506 (2019).
6. M. Jouny, W. Luc, F. Jiao, General techno-economic analysis of CO₂ electrolysis systems. *Ind. Eng. Chem. Res.* **57**, 2165–2177 (2018).
7. C. Xia, Y. Xia, P. Zhu, L. Fan, H. Wang, Direct electrosynthesis of pure aqueous H₂O₂ solutions up to 20% by weight using a solid electrolyte. *Science* **366**, 226–231 (2019).
8. R. F. Service, Renewable bonds. *Science* **365**, 1236–1239 (2019).
9. S. Rebsdat, D. Mayer, in *Ullmann's Encyclopedia of Industrial Chemistry*. (Wiley, 2001).
10. World Petrochemicals Program (WP), "Ethylene," WP Report (SRI Consulting, 2009).
11. World Petrochemicals Program (WP), "Ethylene oxide," WP Report (SRI Consulting, 2009).
12. A. Boulamanti, J. A. Moya, *Energy Efficiency and GHG Emissions: Prospective Scenarios for the Chemical and Petrochemical Industry* (Publications Office of the European Union, 2017).
13. S. T. Wismann, J. S. Engbæk, S. B. Vendelbo, F. B. Bendixen, W. L. Eriksen, K. Aasberg-Petersen, C. Frandsen, I. Chorkendorff, P. M. Mortensen, Electrified methane reforming: A compact approach to greener industrial hydrogen production. *Science* **364**, 756–759 (2019).
14. K. M. Van Geem, V. V. Galvita, G. B. Marin, Making chemicals with electricity. *Science* **364**, 734–735 (2019).
15. H. G. Cha, K.-S. Choi, Combined biomass valorization and hydrogen production in a photoelectrochemical cell. *Nat. Chem.* **7**, 328–333 (2015).
16. N. Jiang, B. You, R. Boonstra, I. M. Terrero Rodriguez, Y. Sun, Integrating electrocatalytic 5-hydroxymethylfurfural oxidation and hydrogen production via Co–P-derived electrocatalysts. *ACS Energy Lett.* **1**, 386–390 (2016).
17. B. You, N. Jiang, X. Liu, Y. Sun, Simultaneous H₂ generation and biomass upgrading in water by an efficient noble-metal-free bifunctional electrocatalyst. *Angew. Chem. Int. Ed.* **55**, 9913–9917 (2016).
18. T. Li, Y. Cao, J. He, C. P. Berlinguette, Electrolytic CO₂ reduction in tandem with oxidative organic chemistry. *ACS Cent. Sci.* **3**, 778–783 (2017).

19. R. S. Sherbo, R. S. Delima, V. A. Chiykowski, B. P. MacLeod, C. P. Berlinguette, Complete electron economy by pairing electrolysis with hydrogenation. *Nat. Catal.* **1**, 501–507 (2018).
20. J. Zheng, X. Chen, X. Zhong, S. Li, T. Liu, G. Zhuang, X. Li, S. Deng, D. Mei, J.-G. Wang, Hierarchical porous NC–CuCo nitride nanosheet networks: Highly efficient bifunctional electrocatalyst for overall water splitting and selective electrooxidation of benzyl alcohol. *Adv. Funct. Mater.* **27**, 1704169 (2017).
21. D. Liu, J.-C. Liu, W. Cai, J. Ma, H. B. Yang, H. Xiao, J. Li, Y. Xiong, Y. Huang, B. Liu, Selective photoelectrochemical oxidation of glycerol to high value-added dihydroxyacetone. *Nat. Commun.* **10**, 1779 (2019).
22. Y. Kwon, Y. Birdja, I. Spanos, P. Rodriguez, M. T. M. Koper, Highly selective electro-oxidation of glycerol to dihydroxyacetone on platinum in the presence of bismuth. *ACS Catal.* **2**, 759–764 (2012).
23. C. Dai, L. Sun, H. Liao, B. Khezri, R. D. Webster, A. C. Fisher, Z. J. Xu, Electrochemical production of lactic acid from glycerol oxidation catalyzed by AuPt nanoparticles. *J. Catal.* **356**, 14–21 (2017).
24. A. Winiwarter, L. Silvioli, S. B. Scott, K. Enemark-Rasmussen, M. Sariç, D. B. Trimarco, P. C. K. Vesborg, P. G. Moses, I. E. L. Stephens, B. Seger, J. Rossmeisl, I. Chorkendorff, Towards an atomistic understanding of electrocatalytic partial hydrocarbon oxidation: Propene on palladium. *Energy Environ. Sci.* **12**, 1055–1067 (2019).
- ~~25. Y. Huang, X. Chong, C. Liu, Y. Liang, B. Zhang, Boosting hydrogen production by anodic oxidation of primary amines over a NiSe nanorod electrode. *Angew. Chem. Int. Ed.* **57**, 13163–13166 (2018).~~
- ~~26. C. Huang, Y. Huang, C. Liu, Y. Yu, B. Zhang, Integrating hydrogen production with aqueous selective semi-dehydrogenation of tetrahydroisoquinolines over a Ni₂P bifunctional electrode. *Angew. Chem. Int. Ed.* **58**, 12014–12017 (2019).~~
- ~~27. Y. Lum, J. E. Huang, Z. Wang, M. Luo, D. H. Nam, W. R. Leow, B. Chen, J. Wieks, Y. C. Li, Y. Wang, C. T. Dinh, J. Li, T. T. Zhuang, F. Li, T. K. Sham, D. Sinton, E. H. Sargent, Tuning OH binding energy enables selective electrochemical oxidation of ethylene to ethylene glycol. *Nat. Catal.* **3**, 14–22 (2020).~~
2825. M. Rafiee, K. C. Miles, S. S. Stahl, Electrocatalytic alcohol oxidation with TEMPO and bicyclic nitroxyl derivatives: Driving force trumps steric effects. *J. Am. Chem. Soc.* **137**, 14751–14757 (2015).
2926. E. J. Horn, B. R. Rosen, Y. Chen, J. Tang, K. Chen, M. D. Eastgate, P. S. Baran, Scalable and sustainable electrochemical allylic C–H oxidation. *Nature* **533**, 77–81 (2016).
3027. M. Rafiee, F. Wang, D. P. Hruszkewycz, S. S. Stahl, N-Hydroxyphthalimide-mediated electrochemical iodination of methylarenes and comparison to electron-transfer-initiated C–H functionalization. *J. Am. Chem. Soc.* **140**, 22–25 (2018).
3128. C. L. McCABE, J. C. Warner, The kinetics of the reaction between the ethylene halohydrins and hydroxyl ion in water and mixed solvents. *J. Am. Chem. Soc.* **70**, 4031–4034 (1948).

3229. M. Eigen, K. Kustin, The kinetics of halogen hydrolysis. *J. Am. Chem. Soc.* **84**, 1355–1361 (1962).
3330. W. Tong, M. Forster, F. Dionigi, S. Dresp, R. Sadeghi Erami, P. Strasser, A. J. Cowan, P. Farràs, Electrolysis of low-grade and saline surface water. *Nat. Energy* (2020).
3431. R. K. B. Karlsson, A. Cornell, Selectivity between oxygen and chlorine evolution in the chlor-alkali and chlorate processes. *Chem. Rev.* **116**, 2982–3028 (2016).
3532. “Market Analytics: Propylene Oxide - 2018,” *Markets & Profitability* (Nexant, 2018).
3633. W. Luc, J. Rosen, F. Jiao, An Ir-based anode for a practical CO₂ electrolyzer. *Catal. Today* **288**, 79–84 (2017).
34. Y. Huang, X. Chong, C. Liu, Y. Liang, B. Zhang, Boosting hydrogen production by anodic oxidation of primary amines over a NiSe nanorod electrode. *Angew. Chem. Int. Ed.* **57**, 13163–13166 (2018).
35. C. Huang, Y. Huang, C. Liu, Y. Yu, B. Zhang, Integrating hydrogen production with aqueous selective semi-dehydrogenation of tetrahydroisoquinolines over a Ni₂P bifunctional electrode. *Angew. Chem. Int. Ed.* **58**, 12014–12017 (2019).
36. Y. Lum, J. E. Huang, Z. Wang, M. Luo, D.-H. Nam, W. R. Leow, B. Chen, J. Wicks, Y. C. Li, Y. Wang, C.-T. Dinh, J. Li, T.-T. Zhuang, F. Li, T.-K. Sham, D. Sinton, E. H. Sargent, Tuning OH binding energy enables selective electrochemical oxidation of ethylene to ethylene glycol. *Nat. Catal.* **3**, 14–22 (2020).
37. “Ethylene Oxide Production by Nippon Shokubai Process,” PEP Review 2010-12 (IHS Markit, 2010).
38. “Ethylene oxide (EO) Prices and Information,” (ICIS, 2011).
39. O. S. Bushuyev, P. De Luna, C. T. Dinh, L. Tao, G. Saur, J. van de Lagemaat, S. O. Kelley, E. H. Sargent, What should we make with CO₂ and how can we make it? *Joule* **2**, 825–832 (2018).

Acknowledgments: We thank **Damir D.** Kopilovic and **Remigiusz R.** Wolowiec for their kind technical assistance. **Funding:** This material is based upon work supported by the Ontario Ministry of Colleges and Universities (Grant ORF-RE08-034), Natural Sciences and Engineering Research Council (NSERC) of Canada (Grant RGPIN-2017-06477), Canadian Institute for Advanced Research (CIFAR) (Grant FS20-154 APPT.2378), and University of Toronto Connaught Fund (Grant GC 2012-13). D.S. acknowledges the NSERC E. W. R. Steacie Memorial Fellowship. **Author contributions:** E.H.S. supervised the project. W.R.L., Y.L., and E.H.S. conceived the idea and designed the experiments. W.R.L and Y.L. carried out all the experimental work. A.O. fabricated the IrO₂-coated Ti mesh electrodes and assisted in the CO₂-to-ethylene oxide conversion experiments. Y.W. performed SEM measurements. D.-H.N. performed the XRD measurements. B.C. carried out the TEM measurements. J.W. carried out the XPS measurements. T.-T.Z., F.L., and D.S. contributed to data analysis and manuscript editing. W.R.L., Y.L., and E.H.S. co-wrote the manuscript. All authors discussed the results and assisted during the manuscript preparation. **Competing interests:** The authors declare no competing interests. **Data and materials availability:** All experimental data are available in the main text or the supplementary materials.

Supplementary Materials

science.sciencemag.org/content/[vol]/[issue]/[page]/suppl/DC1

Materials and Methods

Supplementary Text

Figs. S1 to S12

Tables S1 to S4

References (37–39)

14 October 2019; resubmitted 26 January 2020

Accepted 1 April 2020

Commented [CF7]: Please check your accepted SM file for any citations of references 25-36; if any exist, please send me along with your galley corrections a revised SM file with the in-text reference callouts updated to reflect the new numbering (25 becomes 34, 28 becomes 25, etc.)

Fig. 1. Electrosynthesis of ethylene oxide by using renewable energy. (A and B) Schematics illustrating (A) the industrial thermochemical system and (B) the proposed electrochemical system. (C) Reported current densities and Faradaic efficiencies for other anodic partial oxidation reactions in the literature (blue squares) (15–2724, 34–36). Data for the system demonstrated in this work are shown for comparison (red square). (D) Breakdown of costs at current densities of 50 and 300 mA/cm², as calculated from a ~~technoeconomic analysis (TEA)~~. ~~TEA calculation details are provided in the Refer to S~~ supplementary text and ~~Fig. S1 in the Supporting Materials for TEA calculation details~~.

Fig. 2. Selective ethylene oxide production from ethylene enabled by an extended heterogeneous:homogenous interface. (A) Schematic illustrating ethylene oxidation at planar versus extended interfaces. (B) Schematic of the ethylene-to-ethylene oxide electrochemical system. ~~For A~~ detailed schematic of ~~the electrolyzer~~ ~~see is available in Fig. S3~~. (C) ¹³C NMR spectra of ethylene oxide and ethylene chlorohydrin. (D) Faradaic efficiencies of ethylene oxide and ethylene chlorohydrin at different current densities. (E) Faradaic efficiencies of propylene oxide and propylene chlorohydrin at different current densities. The error bars correspond to the standard deviation of three independent measurements.

Fig. 3. Optimization of energy efficiency to reduce energy cost and maximize technoeconomic benefit. (A) ~~Techno-economic analysis (TEA)~~ showing plant-gate levelized cost as a function of energy efficiency and renewable energy cost. (B) Half-cell energy efficiency and the corresponding plant-gate levelized cost as a function of Cl⁻ concentration. (C) EDX images showing the distribution of Ir, Ti, and O on the IrO₂/Ti mesh. (D) Half-cell energy efficiency and the corresponding plant-gate levelized cost as a function of current density. ~~Note:~~ ~~Our~~ half-cell energy efficiencies are based on our reported potentials ~~vs. versus~~ Ag/AgCl, which are not IR-corrected. Additionally, we assume no losses at the cathode side, where hydrogen evolution occurs. The error bars correspond to the standard deviation of three independent measurements.

Fig. 4. Evaluation of ethylene-to-ethylene oxide performance. (A) Half-cell overpotential and Faradaic efficiency of ethylene oxide over 100 hours at 300 mA/cm². (B) Comparison of current density, product generation rate, reported operation time, Faradaic efficiency, and product selectivity against state-of-the-art anodic upgrading reactions. Specificity refers to the percentage of all reacted substrate going toward the desired product. (C) Schematic of the CO₂-to-ethylene oxide (EO) process in which the ethylene-to-EO cell was directly supplied with the gas output from a CO₂-to-ethylene MEA. (D) Faradaic efficiencies of ethylene (in MEA) and ethylene oxide (in flow cell) as a function of the gas flow rate. For all cases, the MEA was run at 240 mA/cm², and the ethylene oxidation flow cell was operated at 300 mA/cm⁻², for a duration of 1 hour.